Journal of Thermal Analysis and Calorimetry
https://doi.org/10.1007/s10973-024-13003-z

Effect of four-component binder on characteristics of self-compacting and fibre-reinforced self-compacting mortars

Sarella Venkateswara Rao[1,4] · Martin T. Palou[2,3,4] · Radoslav Novotný[3,4] · Matúš Žemlička[2,4] · Jana Čepčianska[2,4] · Peter Czirák[2,4]

Received: 19 August 2023 / Accepted: 19 February 2024

Abstract

The hydration heat of a four-component binder consisting of Portland cement (CEM I 42.5 R), blast-furnace slag (BFS), metakaolin (MK), and silica fume (SF) was investigated using a conduction calorimeter and thermal analytical method to optimize the material composition of self-compacting mortar (SCM). Then, the influence of material composition with different substitution levels (0, 25, 30, and 35% labelled as SCM100, SCM75, SCM70, and SCM65) on physical and mechanical properties of the mortars with two volumetric binder sand ratios of 1:1 and 1:2 (cement: sand) was evaluated. Furthermore, two mortar compositions comprising SCM75 and sand at 1:1 and 1:2 ratios were used to prepare fibre-reinforced self-compacting mortars in five combinations (0, 0.25, 0.5, 0.75, and 1%) of two fibres (polypropylene-PPF and basalt-BF) at a constant content of 1.00 vol%. The properties of the prepared samples were investigated with respect to the characteristics of self-compactibility and mechanical properties of fresh and hardened states, respectively. The rheology characteristics expressed by slump flow, V-funnel, and T20 were found following the EFNARC guidance. The partial replacement of cement by supplementary cementitious materials has enhanced the performances (compressive and flexural strengths, dynamic modulus of elasticity) of self-compacting mortars from the 7th day through pozzolanic activity. Furthermore, adding fibres has enhanced the DME and microstructure of the self-compacting mortars.

Keywords Self-compacting mortars · Supplementary cementitious materials · Hydration heat · Mechanical and physical properties

Introduction

Self-compacting mortars, as advanced building materials, are principally used in the rehabilitation and repair of reinforced concrete structures [1–3]. Placing fresh mortar without any external compaction and at the same time without causing segregation is the main scientific and economic advantage of the development of self-compacting mortars [4]. To meet these specific requirements, the water–cementitious materials ratio of the mortar and the type of chemical admixtures should be determined. In other words, the paste phase rheology of repair mortar should have suitable properties from the viewpoint of flowability and segregation [4, 5]. In addition, the self-compactability of the resulting mortars may provide considerable advantages over conventional mortar such as reducing construction time and labour costs and enhancing the filling capacity of highly congested structural members. High cement content is needed in self-compacting mortars to increase their flowability and stability,

✉ Martin T. Palou
martin.palou@stuba.sk

1 Civil Engineering Department, National Institute of Technology Warangal, Warangal, Telangana 506004, India

2 Institute of Construction and Architecture, Slovak Academy of Sciences, Dúbravská Cesta 9, 84503 Bratislava, Slovak Republic

3 Faculty of Chemical and Food Technology, Slovak University of Technology, Radlinského 9, 81237 Bratislava, Slovak Republic

4 Materials Research Centre, Faculty of Chemistry, Brno University of Technology, Purkyňova 118, 61200 Brno, Czech Republic

Published online: 26 March 2024

and inert fillers and supplementary cementitious materials are usually used for this purpose [6]. An appropriate supplementary cementitious material (SCMs) can be used to improve the segregation resistance of self-compacting mortars while maintaining excellent flowing ability in the fresh state. In fact, most common supplementary cementitious materials such as blast-furnace slag (BFS), metakaolin (MK), and silica fume (SF) have been used to produce self-compacting mortar and self-compacting concrete with good flowing ability [5–11]. On recent developments of concrete and construction materials technology, the study on plastering (with different materials) plays a major role in catering to the issues of crack repairs, damp proofing, and rehabilitation issues of the structures.

Fibre-reinforced SCM is one of the materials widely used to repair old concrete [12]. In the fibre-reinforced SCM, fibres are usually discontinuous and randomly distributed throughout the composite. In the hardened mortar, fibres prevent the microcracks from developing into macrocracks. In addition, these fibres bridge and therefore hold together the existing macrocracks, thus reinforcing the mortar against failure [12]. Likewise in fibre-reinforced concrete, the property enhancement of fibre-reinforced mortar can be largely attributed to the crack bridging forces provided by the fibres, which limit crack opening and distribute the stresses to the nearby matrix, thus suppressing strain localization [13–15]. Consequently, the strength and strain capacity of the composite increased appreciably. Hybrid fibre-reinforced self-compacting mortar gives the advantage of two or more than two types of fibres that can be added in self-compacting mortar. It improves the properties of single fibre-reinforced self-compacting mortar. Hybrid fibre-reinforced self-compacting mortar is a new composite material produced by adding different types, shapes, and dimensions of fibres in a self-compacting mortar.

The use of fine mineral admixtures in SCMs is inevitable to enhance their self-compactibility characteristics and reduce self-compacting concrete's material cost (SCC). Self-compacting mortar (SCM) may serve as a basis for the design of concrete, and the properties of SCMs highlight the workability of SCC mixtures. According to Domone and Jin [9], mortars are being tested for the following reasons: SCC has a lower coarse aggregate content than that of normal concrete (typically 31–35% by volume), and therefore, the properties of the mortar are dominant. Assessing the properties of the mortar is an integral part of many SCC mix design processes; therefore, knowledge of the properties is useful. The combination of powder materials is also used to control the hardened properties, such as strength. Testing mortar is more convenient than testing concrete. Studies on the paste or mortar have shown that the rheological properties of the matrix are important to achieve the required fresh properties of SCC. Due to the lower content of coarse aggregate in SCC, mortar exerts more effects on the fresh properties of SCC than conventional concrete (CC). Mortar not only provides lubrication by wrapping coarse aggregates, but it also predominantly influences the fresh properties of SCC with a low yield stress and adequate viscosity so as to ensure the required filling and passing ability without blocking and segregation. Mortar is, thus, an integral part of SCC mix design. Hence, self-compacting mortar (SCM) is a precondition for the successful production of SCC. To enhance the rheological properties, the binder composition of the self-compacting mortars should be optimized based on the particle size distribution and mainly on hydration heat. Indeed, the rapidity and quantity of heat evolved could influence the binder past flowability by forming hydration products that cause the setting and hardening of fresh mortars. Therefore, hydration heat and hydration products should be determined before the determination of the material composition. According to general knowledge, the hydration of blended cement containing various supplementary cementitious materials [16] should be governed by the principle of OPC hydration, alkali-activation, or pozzolanic reactions. In recent decade, several authors [17–21] have undertaken suitable works to understand the effect of ground granulated blast-furnace slag, metakaolin, silica fume, and limestone on the hydration of multicomponent cementitious binders. Systems comprising Portland cement and the addition of one, two, three, or four supplementary cementitious materials with substitution levels reaching 35% by mass of cement were deeply investigated. The concomitant dilution (due to the replacement of Portland cement by SCMs) effect and pozzolanic reactions were examined at laboratory conditions. It was found that the presence of supplementary cementitious materials has an impact on the dissolution of C_3S due to their affinity towards calcium hydroxide. First, PC should react with water to release calcium hydroxide, which serves to initiate the secondary alkali-activated or pozzolanic reactions. As hydration is a complex process extended over time, the mutual influence of alkali-activation and the primary hydration of PC were observed.

The substitution of Portland cement clinker with reactive supplementary cementitious materials and limestone is currently the primary lever for reducing the carbon footprint of cement manufacture, and this is projected to be the case for decade to come.

The main objective of this work is to study the strength and microstructure characteristics of self-compacting and fibre-reinforced self-compacting mortar (SCM) using four-component binders (cement, GGBS, metakaolin, and silica fume) with two volumetric binder sand ratios of 1:1 and 1:2, and three kinds of fibres.

Experimental

The standardized cement–sand ratio is 1:3 for mortars, but in the case of self-compacting mortars, this ratio may vary depending on the required rheological properties. The four combinations of binders in SCM mixes are listed in Table 2, and the mix composition for SCM(1:1) and SCM (1:2) are depicted in Table 3 and Table 4, respectively. After determining the hydration heat and self-compactibility, specimens of 4 cm × 4 cm × 16 cm size were cast; compressive and flexural strengths, dynamic modulus of elasticity (DME) for SCM(1:1) and SCM(1:2) mixes were tested at 2, 7, and 28 days. Then, ten specimens of fibre-reinforced mortars based on SCM75(1:1) and SCM(1:2) with different combinations of polypropylene (PPF) and basalt (BF) fibres were prepared. The five combinations of fibres in SCM(1:1) and SCM(1:2) mixes are designated as follows: SCM75A(0% PPF and 1% BF), SCM75B(0.25% PPF and 0.75% BF), SCM75C(0.5% PPF and 0.5% BF), SCM75D(0.75% PPF and 0.25% BF), and SCM75E(1% PPF and 0% BF).

Testing procedures

The rheological characteristics of self-compactibility were determined following EFNARC(details are reported in 2.1. Test methods). Dynamic modulus of elasticity (DME) was conducted at 2, 7, and 28 days. The hydration reaction of the binders and the characteristics of hydration products were investigated using a conduction calorimeter TAM AIR 8–Channel calorimeter as described elsewhere [18, 19]. After that, the phase changes were examined by TGA/DSC technique (TGA/DSC–1, STARe software 9.30, Mettler Toledo). The 50.00 (± 0.03) mg of powdered samples was heated in the open platinum crucibles up to 1000 °C at the heating rate of 10 °C min^{-1} in N_2 atmosphere. The chemical composition of used materials determined by means of energy-dispersive X-ray fluorescence (EDXRF) method using SPECTRO XEPOS HE Spectrometer is reported in Table 1. The microstructure observation was carried out using the JSM-6610A (JEOL, Tokyo, Japan) scanning electron microscopy (SEM) with a conventional tungsten filament. The compressive strength of samples was tested using WPM WEB Thuringer Industriwerk Rauestein 11/2612 (up to 25 000N) at 2, 7, and 28 days. Each displayed data represents the arithmetic mean of six experimental measurements. Dynamic modulus of elasticity (DME) was conducted at 2, 7, and 28 days using UPV method.

Table 1 Chemical composition of cementitious materials (% by mass)

Chemical element	Cement (CEM I 42.5 R)	GGBS	Metakaolin	Silica Fume
SiO_2	19.10	37.20	53.70	97.10
Al_2O_3	4.43	8.50	39.90	0.21
Fe_2O_3	2.60	0.24	1.15	–
CaO	63.80	38.90	0.45	0.50
MgO	2.39	10.20	0.30	0.40
TiO_2	0.25	0.30	1.42	
MnO	0.19	0.51	< 0.01	
K_2O	0.53	0.36	0.74	
Na_2O	0.41	0.46	0.07	
P_2O_5	0.09	0.02	0.08	
SO_3	3.49	3.01	0.11	-
Cl^{-1}	0.09	0.03	< 0.01	
BaO	0.03	0.08	0.04	
SrO	0.02	0.06	0.02	
Loss by ignition	2.31	0.36	1.75	

Materials

The materials used in this study were selected taking into consideration their quality. The following materials were therefore used:

- Cement type I—42.5 R with specific surface area of 4341 $cm^2 \cdot g^{-1}$ was from Danucem (former CHR) Rohožník, Slovak republic
- Reactive alkaline GGBS with 78% of glass content and with specific surface area of 4275 $cm^2 \cdot g^{-1}$ was from Moravia Steel, JSc., Třinec, Czech Republic.
- Metakaolin MK Mefisto K05 with specific surface area of 2586 $cm^2\ g^{-1}$ was from České lupkové závody, a.s.,
- Silica fume (SF) with specific surface area of 15,000 $cm^2 \cdot g^{-1}$ was fromOravské ferozliatinárske závody, a.s., Slovakia.
- Three siliceous sands of 0/1, 1/2, and 2/4 sizes.
- STACHEMENT 2000 as a superplasticizer based on polycarboxylates with high plasticizing effect was used in this study.
- Three kinds of fibres (basalt, carbon, and PP) with determined modulus of elasticity, tensile strength, diameter, and length were used to prepare fibre-reinforced self-compacting mortar.
- Tap water was used for both casting and curing of the specimens.

Test methods of EFNARC

Mortar tests are widely used to design and evaluate SCC mixes. Assessing the properties of SCM is an integral part of SCC design. EFNARC (European Federation of National Trade Associations) is the only available standard that is dedicated to special construction chemicals and concrete systems. It describes various tests involved in mortar tests to determine the optimum w/cm and optimum dosage of SP in mortar. They are the mini-slump cone test to measure the relative slump of the mortar and the mini-V-funnel test to measure the flow rate or viscosity of the mortar.

Mini-slump cone and graduated glass plate

The test apparatus for measuring the spread and viscosity of mortar comprises a mini-frustum (slump) cone and a graduated glass plate. Mini-slump cone has top and bottom diameters of 7 cm and 10 cm, respectively, with a cone height of 6 cm. The graduated glass plate contains two circular graduations of 10 cm and 20 cm in diameter marked at the centre of the glass plate, as shown in Fig. 1a. With this test apparatus, both viscosity and spread of the mortar can be measured from a single test.

Determination of spread

In this test, the truncated cone mould is placed exactly on the 10 cm diameter graduated circle marked on the glass plate, filled with mortar and lifted upwards. The subsequent diameter of the mortar is measured in two perpendicular directions, and the average of the diameters is reported as the spread of the mortar.

Determination of T_{20}

T_{20} is the time measured from lifting the cone to the mortar reaching a diameter of 20 cm. The measured T_{20} indicates the deformation rate or viscosity of the mortar. So, during this test, T_{20} can be measured first and average of the spread can be measured subsequently. This procedure is similar to slump cone test conducted on SCC.

V-funnel test

The V-funnel flow test for SCM is also described by EFNARC as shown in Fig. 1b. The funnel is filled completely with mortar, and the bottom outlet is opened, allowing the concrete to flow. The flow of mortar is the elapsed time (t) in seconds between the opening of the bottom outlet and the time when the light becomes visible from the bottom, when observed from the top.

Preparation of mortar standard samples

Casting

Standard moulds of size 40 mm × 40 mm × 160 mm were casted which are used for compressive and flexural tests at the age of 2, 7, and 28 days.

Curing

After the completion of the casting, all the specimens were cured in ambient conditions of 20 ± 2 °C and 90% relative humidity for 24 h. The specimens were removed from the mould and submerged in clean, fresh water until just prior to testing. The temperature of water in which the cubes were

(a) Mini slump cone apparatus **(b)** Mini V-funnel apparatus

Fig. 1 **a** Mini-slump cone apparatus, **b** Mini-V-funnel apparatus

submerged was maintained at 20 ± 2 °C. The specimens were cured for 28 days.

Compressive and flexural strength tests

This test was performed at 2, 7, and 28 days. For that purpose, 40 mm × 40 mm × 160 mm moulds were used, which were kept in a wet chamber (20 ± 2 °C and RH ≥ 95%) after de-moulding at 24 h. The specimens were tested immediately after having been taken from the curing chamber. The test was performed in three moulds for each reference and test age with a 3000 kN hydraulic press and a loading rate of 0.6 ± 0.2 MPa·s^{-1} (N·mm^{-2}·s^{-1}).

The compressive strength is given by Eq. (1):

$$f_c = \frac{F}{A_c} \tag{1}$$

in which: f_c = compressive strength (N·mm^{-2}); F = maximum load at failure (N), and A_c = cross-sectional area of the specimen (mm^2).

The flexural strength is given by Eq. (2)

$$F_t = \frac{3Fl}{2bd^2} \tag{2}$$

in which: F_t= flexural strength (N·mm^{-2}); F = maximum load at failure (N), $l = c/$ length of support (mm), b = breadth of the specimen (mm) and d = depth of the specimen (mm).

Dynamic elasticity modulus

This test was based on measuring the propagation time of ultrasonic wave pulses through the given material. Measurements were carried out using the TICO ultrasonic instrument with external 150-kHz probes (the frequency was chosen in view of the dimensions of the specimens). The value of the dynamic elasticity modulus E_u in compression and tension in N/mm^2 can be ca1culated from the formula:

$$E_u = \rho.V_L^2.\frac{l}{k^2}.10^{-6} \tag{3}$$

$$V_L = \frac{L}{t} \tag{4}$$

V_L= Propagation velocity of the ultrasonic pulse (m/sec).
L= Length of the specimen (mm).
t= measured time of passage of ultrasonic pulse (µsec).
ρ= Bulk density of SCM mortars (kg·m^{-3}).
k = a dimensionless coefficient characterizing the size of the specimens.

Results and discussion

Hydration reaction of the four-component binder

As a versatile method, conduction calorimetry is used to record continuously and in real time the heat flow of the exothermic hydration reaction of cementitious materials. Cumulative heat and total hydration heat outputs are calculated using measured heat flow. Then, the data are used to characterize the kinetics and mechanism of hydration reaction and to investigate the influences of different factors, such as

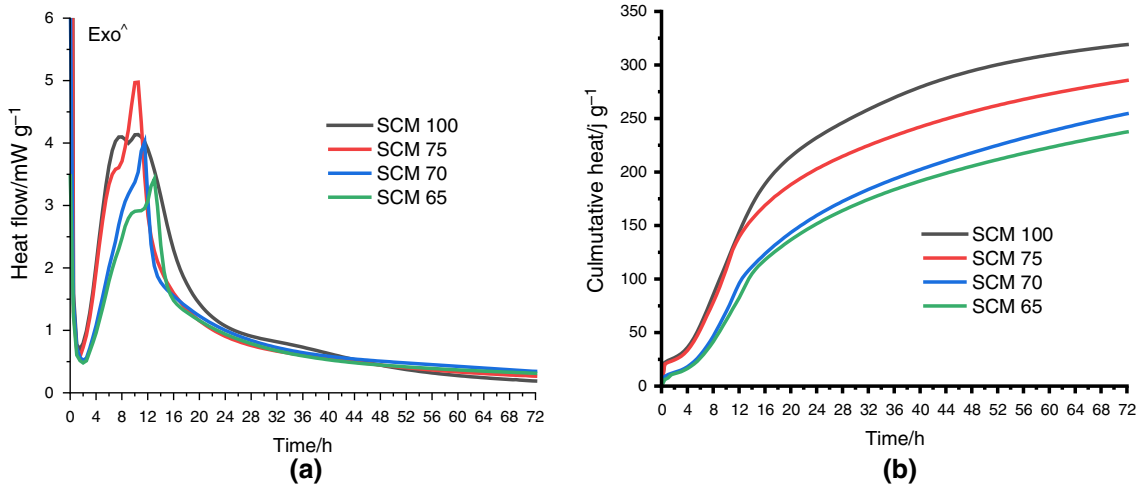

Fig.2 Heat flow and cumulated hydration heat during the first 72 h

temperature, admixtures, and fineness, upon the hydration and physical properties of cement paste, mortars, and concretes [17, 22–24]. The heat flow and cumulated hydration heat during the first 72 h hydration of the four-component binder are shown in Fig. 2a, b. Calorimetric curves were deeply discussed by different authors [23–25]. According to the general knowledge, three main exothermic peaks with four main stages (dissolution, induction, acceleration, and deceleration) can be observed at the curves of the hydration heat flow of all samples. The initial peak within the first hour corresponds to the exothermic physical processes such as wetting and dissolution and chemical reaction of C_3A with gypsum ($CaSO_4.2H_2O$) to form the first ettringite by topochemical process, causing the induction period after forming a protective layer. The first observed peak after the induction period is due to the hydration of C_3S, resulting in nucleation and crystallization of C–S–H and CH. The intensity of this peak decreases with decreasing content of cement in the blends. The phenomenon is called the "dilution effect". Also, the cumulative hydration heat decreases with cement content. Then, shoulder or second peak after the main one appears. It is generally attributed to the second exothermic reaction related to C_3A (formation of ettringite after depletion of the protective layer or decomposition of ettringite into monosulfate) [20, 21]. But, the second peak becomes sharper and more intensive with increasing the substitution level. The alkali-activated reaction of SCMs with a high content of aluminium bearing materials supports the formation of ettringite in the presence of an excess of gypsum [18]. Indeed, metakaolin or blast-furnace slag can, after dissolution, contribute to the formation of ettringite or monosulphate, as reported by [18, 25, 26].

TG/DTG analysis

The TG curve (Fig. 3a) shows the overall loss of water physical and chemically bonds during hydration and can serve to characterize quantitatively different hydration products. The total mass loss is related to the substitution level and material composition. Even if the substitution level varies from 25 to 35%, the composition of supplementary cementitious materials plays a primordial role. Indeed, BFS, SF, and MK have different alkali-activation capacities. Moreover, they are of different specific surfaces, contributing to the reaction rate. The pozzolanic reaction or alkali-activated reactions of BFS, SF, and MK were deeply investigated and broadly reported in the literature [19, 20, 27, 28].

DTG curve (Fig. 2b) serves to qualitatively characterize the presence of products formed during hydration, including carbonization. The peaks found below 100 °C denote the presence of humidity or water physically bound. After 72 h of calorimetric tests, the samples were immediately analysed. The presence of a peak denoting the presence of water physically bound has no effect on the type and intensity of further endothermic peaks. The temperature interval to 300 °C characterizes the presence of C–S–H and ettringite, with the peak at around 110 °C and C–A–S–H at 180 °C. The main characteristic of pozzolanic activity is illustrated by a peak denoting the presence of calcium hydroxide and located in 400–500 °C [19, 20]. An important part of calcium hydroxide has been used in the alkali-activation reaction providing additional hydrated products. The primary hydration reaction and pozzolanic ones were in detail reported by numerous authors [20, 21, 27–29], where some TG measurements were used to determine the degree

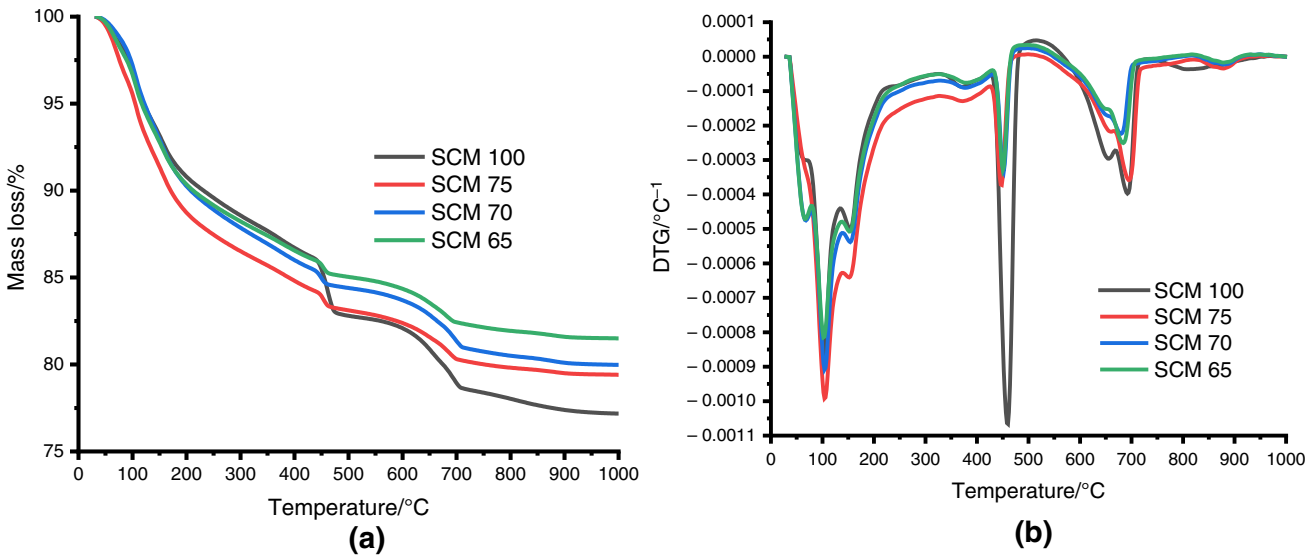

Fig.3 TG (**a**) and (DTG) curves of four-component binder after 72 h

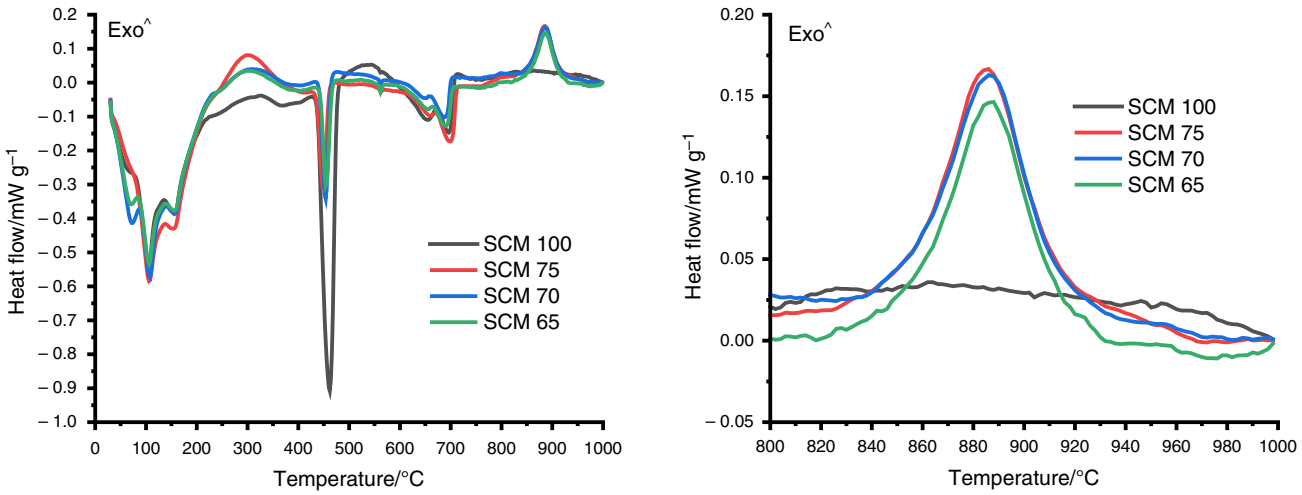

Fig.4 DSC curves (**a**) and detail of DSC within interval 800–1000 °C (**b**) of four-component binder after 72 h

of calcium consumption in the alkali-activation reaction of cement.

The formation of additional hydrated products has caused an increase in mechanical strength, which exceeds that of referential mortar even at 7 days in some cases. The last peaks observed at intervals 600–1000 °C reveal the presence of different kinds of calcium carbonate resulting from different degrees of crystallization of carbonated products.

The contribution of supplementary cementitious materials to the formation of additional hydrated products can be proved by the DSC curve (Fig. 4a) with an exothermic peak located at around 900 °C. A more detailed study reported by [18] has shown the formation of wollastonite and gehlenite. Indeed, wollastonite results from the thermal decomposition of C–S–H with C/S ≅ 1 when supplementary calcium is involved in the reaction. Calcium hydroxide participates actively in the formation of calcium–silicate–hydrate (C–S–H) and calcium–aluminium–silicate–hydrate (C–A–S–H) through a pozzolanic reaction with silica fume and metakaolin. The principle of the pozzolanic activity of materials primarily comprising silica and reactive alumina is based on the model reported in [29]. The activation occurs by sequences of conjoined reactions basing on destruction–coagulation–condensation–crystallization mechanism. Though the thermal decomposition of gehlenite hydrate occurs at 180 °C, the rearrangement of its structure to crystalline one is done at 900 °C with an exothermic effect (Fig. 4b).

The pozzolanic reaction is illustrated by the DTG curve where the peak velocity denoting the endothermic decomposition of calcium hydroxide in a mortar containing supplementary cementitious materials is drastically reduced compared with that of referential mortar. The reduction of $Ca(OH)_2$ peak velocity pastes indicates its consumption in the pozzolanic activity. As the content of supplementary cementitious materials increases (i.e. the higher addition of SCMs), the higher the content of amorphous SiO_2 is available to react with $Ca(OH)_2$. This reaction is more effective with the large amount of $Ca(OH)_2$, which comes from the hydration of C_3S and C_2S to produce C–S–H.

The hydration of self-compacting mortars has the same characteristics as hydration of ordinary mortars or cement paste with the same binders. The main difference lies in the composition of the binder, binder-to-filler ratio, water-to-binder ratio, and additive to prepare self-compacting mortars meeting the requirements of EFNARC guidelines [30]. In the development of the self-compacting mortar, emphasis is placed on the rheological properties, the pozzolanic effect responsible for developing higher strength at a later age, the compactness of the microstructure, and the refinement of the pore structure [30–33].

Rheological properties of four-component binders

This study considered two mixes (1:1 and 1:2) of self-compacting mortars (SCM) with four-component binders

Table 2 Composition of four-component binders

	Cement (CEM I 42.5 R)	GGBS	Metakaolin	Silica Fume
SCM 100	100	–	–	–
SCM 75	75	5	5	15
SCM 70	70	10	10	10
SCM 65	65	15	15	5

Table 3 Mix proportions of SCM(1:1) mixes with component binders

Mix (1:1)	Cement/kg m^{-3}	GGBS/kg m^{-3}	MK/kg m^{-3}	SF/kg m^{-3}	FA I/kg m^{-3}	FA II/kg m^{-3}	FA III/kg m^{-3}	Water/kg m^{-3}	w/b	SP (% bwc)
SCM 100	976.56	–	–	–	325.52	325.52	325.52	410.2	0.42	0.45
SCM 75	732.42	48.83	48.83	146.48	325.52	325.52	325.52	410.2	0.42	0.60
SCM 70	683.59	97.66	97.66	97.66	325.52	325.52	325.52	410.2	0.42	0.60
SCM 65	634.76	146.48	146.48	48.83	325.52	325.52	325.52	410.2	0.42	0.60

Table 4 Mix proportions of SCM(1:2) mixes with component binders

Mix (1:2)	Cement/kg m^{-3}	GGBS/kg m^{-3}	MK/kg m^{-3}	SF/kg m^{-3}	FA I/kg m^{-3}	FA II/kg m^{-3}	FA III/kg m^{-3}	Water/kg m^{-3}	w/b	SP (% bwc)
SCM 100	781.25	–	–	–	520.83	520.83	520.83	328.1	0.42	0.60
SCM 75	585.95	39.06	39.06	117.18	520.83	520.83	520.83	328.1	0.42	0.80
SCM 70	546.86	78.13	78.13	78.13	520.83	520.83	520.83	328.1	0.42	0.80
SCM 65	507.83	117.18	117.18	39.06	520.83	520.83	520.83	328.1	0.42	0.80

Table 5 Fresh properties of 1:1 SCM with biding materials

Mix (1:1)	Slump Flow / mm	T_{20} /sec	V-Funnel/sec
SCM100(1:1)	290	2.19	7.54
SCM75(1:1)	275	2.56	8.36
SCM70(1:1)	265	3.05	8.53
SCM65(1:1)	260	3.24	9.26

Table 6 Fresh properties of 1:2 SCM with binding materials

Mix (1:2)	Slump Flow/ mm	T_{20}/sec	V-Funnel/sec
SCM100(1:2)	285	2.28	7.86
SCM75(1:2)	265	3.53	8.57
SCM70(1:2)	258	4.35	9.82
SCM65(1:2)	245	4.82	10.04

(cement, GGBS, metakaolin, and silica fume). The mix proportions are shown in Tables 3 and 4. The properties of the two fresh SCM mixes are evaluated using mini-slump and mini-V, and the results are reported in Tables 5 and 6.

Tables 5 and 6 report the experimental results for the slump flow diameters, T_{20}, and V-funnel flow times. It is evident that the diameter of slump flow decreases with increasing content of supplementary cementitious materials. On the contrary, T_{20} and V-funnel flow times increase with increasing substitution levels, in other words, with increasing content of supplementary cementitious materials. Higher times V-funnel tests mean less workability and lower filling ability. As per EFNARC guidelines, all the SCM mixes have a slump flow of 240–260 mm and a V-funnel time of 7–11 s. The same findings were reported by [3–10].

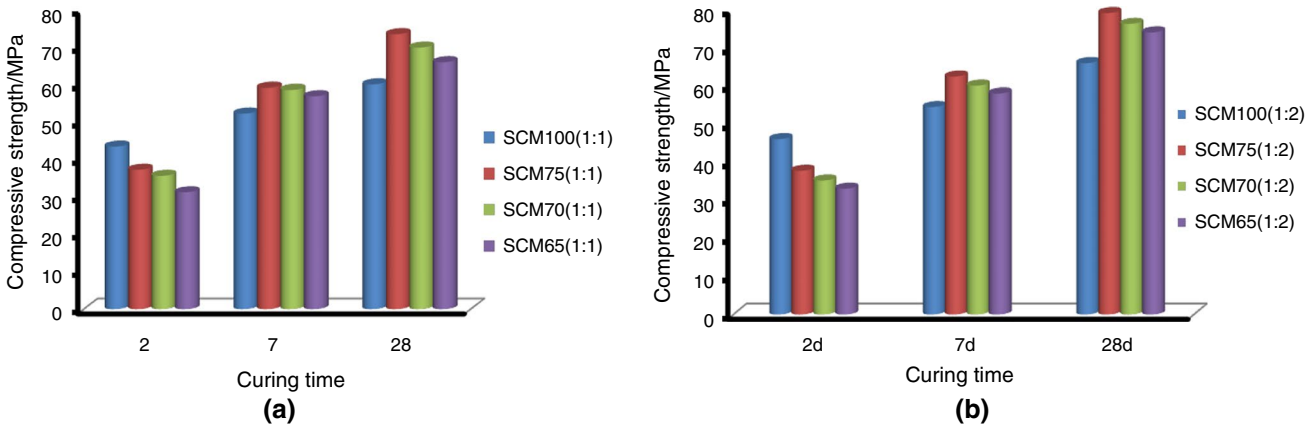

Fig.5 Compressive strength of **a** SCM(1:1) and **b** SCM(1:2)

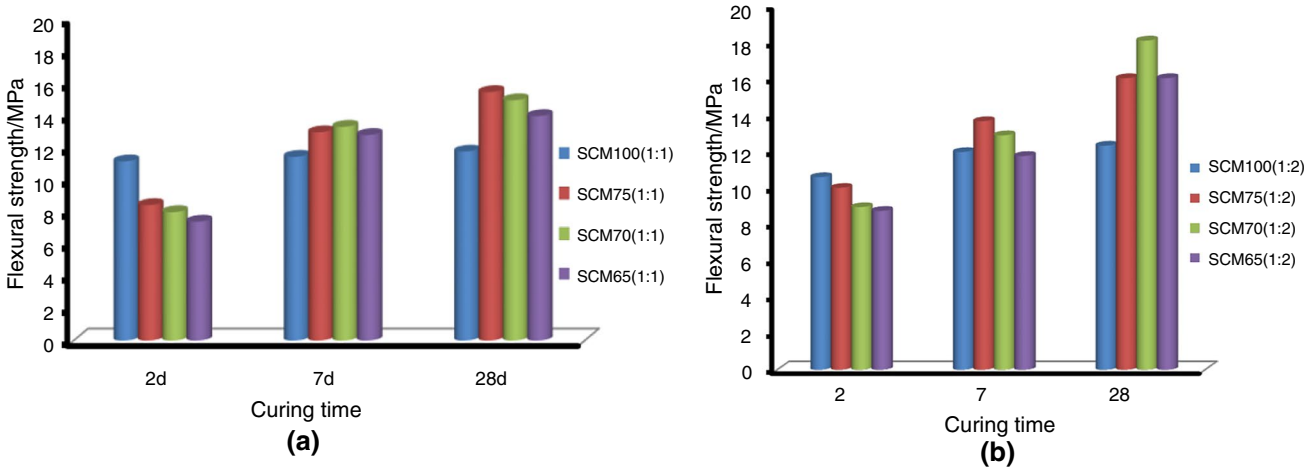

Fig.6 Flexural strength of **a** SCM(1:1) and **b** SCM(1:2)

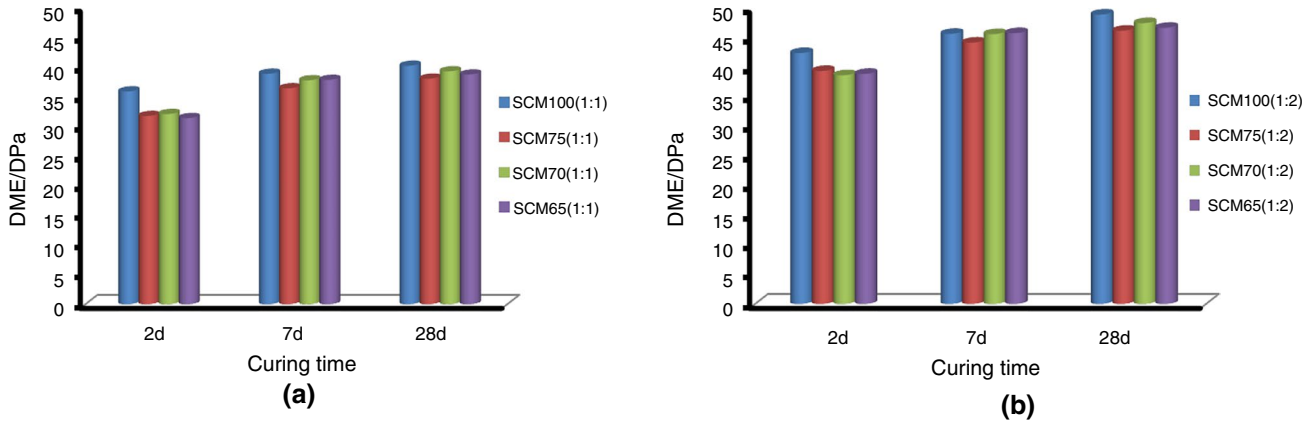

Fig.7 Dynamic modulus of elasticity of **a** SCM(1:1) and **b** SCM(1:2)

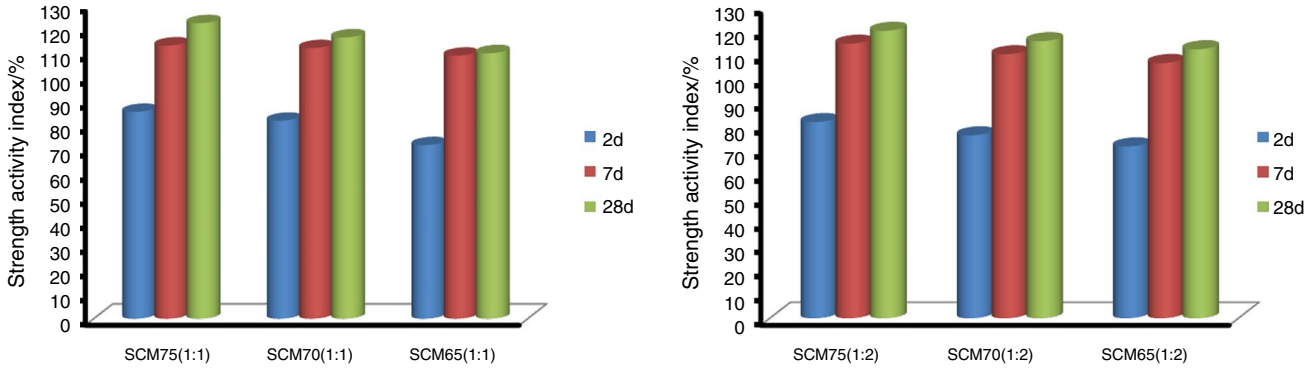

Fig. 8 Strength activity index (SAI) of SCM(1:1) and SCM(1:2) at different substitution levels

Mechanical properties

Compressive, flexural strengths, and dynamic modulus of elasticity

Strength properties like compressive, flexural strengths, and dynamic modulus of elasticity (DME) tests were conducted at the ages of 2, 7, and 28 days of water curing for SCM(1:1), and SCM(1:2) with different binder ratios are depicted in Figs. 5–8. One can observe the variation of compressive, flexural strengths, and dynamic modulus of elasticity of SCM(1:1), and SCM(1:2) at the age of 2, 7, and 28 days. It is evident that the material composition plays a key role in the development of mechanical properties. The substitution levels coupled with silica fume content made SCM75 have higher compressive and flexural strengths than SCM70 and SCM65 in both mixes (Fig. 5a, b) at 7 and 28 days.

The reference mortar samples SCM100(1:1) and (b) SCM100(1:2) prepared with 100 mass% of cement reached the highest compressive and flexural strength on the second day of curing and became the lowest from the 7th. The binder composition has a decisive influence on the development of mechanical properties. Indeed, the cement replacement level by supplementary cementitious materials causes the decrease of mechanical strength at 2-day curing proportionally and vis-à-vis that of the control sample (Figs. 5, 6a, b). After the 7th and 28th, these values, though depending on binder composition, exceed that of the control SCM100. Performance of mechanical properties is observed in samples SCM(1:2) also. Indeed, the mechanical properties of self-compacting mortars with high filler content (SCM(1:2)) are higher than that of SCM(1:1). The higher values of compressive strength in SCM(1:2) could come from the content of sand, reduced amount of water, and the increased superplasticizer content to meet the requirement of rheology defined by EFNARC. If the general school of ideas confirms that the evolution of mechanical properties depends on hydration degree, the absolute values of compressive are influenced by the binder/filler ratio in mortars. Therefore, the strength activity index (SAI), coefficient of pozzolanic activity (CPA), and Pozzolana Effectiveness Coefficient (PEC) are afterwards used to explore the performance of pozzolanic reaction on the mechanical properties.

The chemical reaction of cement binder performs the mechanical and physical properties of mortars. Two main classes of reactions are considered when using SCMs to replace cement: (1) the primary hydration providing C–S–H, ettringite, and calcium hydroxide; (2) the alkali-activation reaction (pozzolanic reaction) of calcium hydroxide with supplementary cementitious materials leading to the formation of additional hydrated products.

The dilution effect due to the replacement level and pozzolanic reaction due to the alkali activation are the two factors that govern the evolution of mechanical properties. At an early curing period, the cement content is decisive for an increase of mechanical properties, while at altering age; the effect of pozzolanic reaction overcomes that of replacement level resulting from the synergetic effects.

DME, which expresses mortar stiffness, is an excellent indicator of the strength and durability of mortars under cyclic loading. As shown in Fig. 7a, b, the DME of SCM(1:1) and (b) SCM(1:2) mortars ranges from 30 to 50 GPa and depends on the sand content rather than the composition of the material at the given test age. The DME varies slightly with the composition of the mixture. However, the DME of the reference sample slightly higher compared with the other samples during the test time. It is generally recognized that mortars with a higher DME can withstand more stress before becoming brittle.

Strength activity index and coefficient of pozzolanic activity

The strength activity index expresses the ratio between absolute values of compressive strength of mortar samples prepared with a certain level of substitution by supplementary cementitious materials and that of referential mortar considered (Eq. 1). Values less than 100% mean that the compressive strength of the samples is always less than that of the reference, while values greater than 100% prove that the compressive strength of the samples exceeded that of the reference. According to European standard EN 450 and ASTM C618 standard, supplementary cementitious materials are only allowed to be used as pozzolanic material in concrete if strength activity indexes are more than 75% at 28 days and 85% at 90 days compared to reference concrete.

$$\mathrm{SAI} = \frac{\mathrm{Cs}_{\mathrm{SCM}}}{\mathrm{Cs}_{\mathrm{Ref}}} \times 100 \tag{5}$$

The strength activity index of the SCM75, SCM70, and SCM65 for both mixes at each specific curing time is depicted in Fig. 8. Both groups of samples show the SAI higher than 75% even after 2 days and higher than 100% after 7 and 28 days. The strong SAI of samples with replacement levels to 35% indicates the possibility to extent the amount of supplementary cementitious materials. However, these extensions are limited by the requirements for self-compactibility rather than SAI.

Coefficient of pozzolanic activity (CPA; in %)

In order to characterize the effect of substitution level and pozzolanic activity on the mechanical properties of mortars in relation to reference one, the so-called coefficient of pozzolanic activity (CPA; in %) according to Eq. 7 is used. This relationship serves to determine the mutual effect of dilution and pozzolanic reaction and was used by authors [18, 34]. The coefficient of pozzolanic activity measures the real contribution of the pozzolanic activity of supplementary cementitious materials to the strength development and characterizes the mutual effect of dilution and pozzolanic reaction. Therefore, the contribution of supplementary cementitious materials can be calculated keeping in consideration the theoretical reduction of compressive

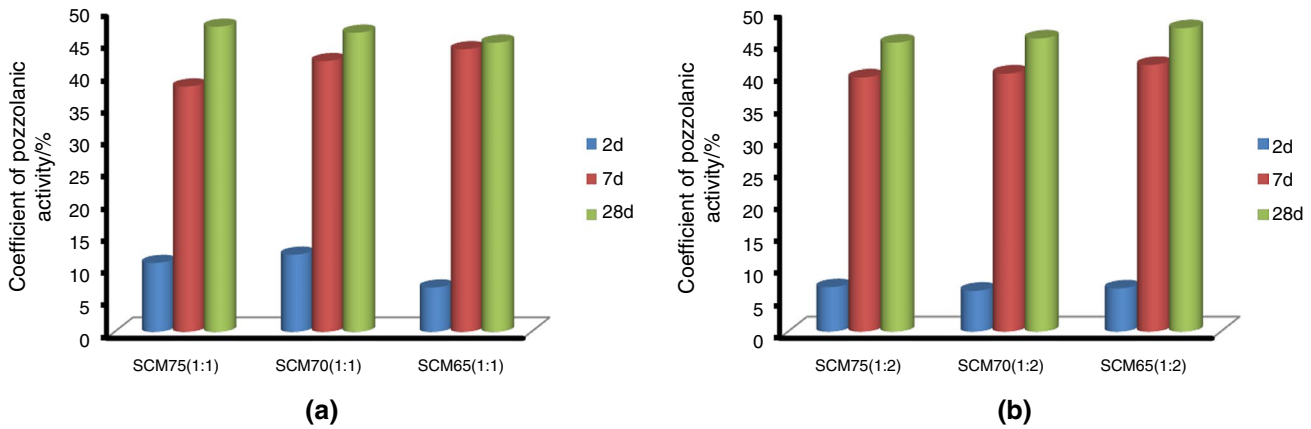

Fig. 9 Coefficient of pozzolanic activity (CPA) of SCM(1:1) and SCM(1:2) at different substitution levels

strength due to the replacement level (dilution effect) and the real compressive strength measured at the determined curing time.

$$(\mathrm{CPA})_x = \frac{\mathrm{Cs}_{\mathrm{SCM}} - \left(1 - \frac{\chi}{100}\right) C_{\mathrm{Ref}}}{C_{\mathrm{Ref}}} \quad (6)$$

$(\mathrm{CPA})_x$ represents the coefficient of pozzolanic activity of the sample at curing time x, C_{Ref} is the compressive strength of mortar reference, $\mathrm{Cs}_{\mathrm{SCM}}$ the compressive strength of the particular mortar sample at a corresponding curing time ×, χ is the substitution level (25, 30, and 35%) corresponding to SCM75, SCM70, and SCM65.

Figure 9a, b shows that at the earlier period of curing (2 days), the contribution of the alkali-activated reactions to the development of compressive strength varies from 6 to 12% in both mixes SCM(1:1) and SCM(1:2) and increases with curing time to attain 45–48% at 7 and 28 days. While the substitution level varies from 25 to 35%, the contribution of alkali-activated reactions to the strength development varies from 45 to 48% at 28 days. It tends to increase over time due to the synergetic effect of hydration and pozzolanic reactions.

Pozzolana Effectiveness Coefficient (PEC)

Zaleska et al. [35] have introduced a new method; the so-called Pozzolana Effectiveness Coefficient (PEC), as shown in Eq. (8) to characterize the mutual contribution of pozzolana and cement to the strength to more clearly define the effectiveness of a specific amount of pozzolana in the blend.

$$(\mathrm{PEC})_x = \frac{\mathrm{Cs}_{\mathrm{SCM}} - \left(1 - \frac{\chi}{100}\right) C_{\mathrm{Ref}}}{\left(\frac{\chi}{100}\right) C_{\mathrm{Ref}}} \quad (7)$$

$(\mathrm{PEC})_x$ represents the Pozzolana Effectiveness Coefficient (PEC) of the sample at curing time x, C_{Ref} is the compressive strength of mortar reference, Cs_{SCM} the compressive strength of mortar sample at a corresponding curing time ×, χ is the substitution level (25, 30, 35) corresponding to SCM75, SCM70, and SCM65. This method was used by [35] to characterize the strengthening effect of fly ash in cement after 28 days of curing. To prove that the new method can be reasonably and effectively used to characterize the impact of the addition of pozzolana on the mechanical properties of cement-based materials, the classification of a pozzolana using PEC is done as follows:

a) $(\mathrm{PEC})_x < 0$—the analysed material cannot be considered as a pozzolana, it acts as a filler only,
b) $0 < (\mathrm{PEC})_x < 1$—the analysed material, in a blend with Portland cement, acts as a pozzolana; the higher is the PEC value, the higher is the pozzolanicity,
c) $(\mathrm{PEC})_x > 1$—the effectiveness of the pozzolana is higher than Portland cement, there are synergetic effects in the Portland cement pozzolana-water system.

The PEC of the mixtures, calculated according to Eq. 7, is depicted in Fig. 10a, b. The values are comprised between 0 and 1 at 2nd day and significantly exceed 1 at 7th and 28th day, depending on the material composition. But, the PEC decreases with decreasing content of cement. Indeed, the dilution effect reduces the $Ca(OH)_2$ necessary for the pozzolanic reaction in an aqueous medium. In addition, it is worth noting that the solidification of the paste structure causes the reduction of the mobility of the ions and, consequently, will slow down the development of mechanical properties. But, the compressive strength of mixes with high content of supplementary cementitious materials can develop slowly and exceed over time that of samples with high cement content.

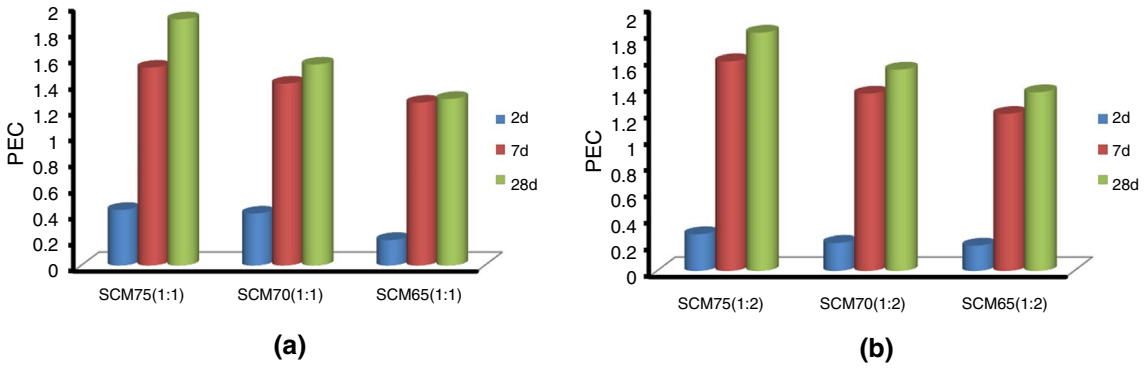

Fig.10 The Pozzolana Effectiveness Coefficient (PEC) of SCM(1:1) and SCM(1:2) at different substitution levels

Table 7 Fresh properties of fibre-reinforced SCM75(1:1) mortars

Mix (1:1)	Slump Flow/mm	T_{20}/s	V-Funnel/s
SCM75(1:1)A	280	3.05	6.85
SCM75(1:1)B	250	3.44	9.35
SCM75(1:1)C	258	3.12	9.74
SCM75(1:1)D	264	3.27	10.06
SCM75(1:1)E	260	3.64	10.26

Table 8 Fresh properties of fibre-reinforced SCM75(1:2) mortars

Mix (1:2)	Slump Flow/mm	T_{20}/s	V-Funnel/s
SCM75(1:2)A	265	3.25	8.07
SCM75(1:2)B	264	3.62	9.10
SCM75(1:2)C	258	3.93	9.97
SCM75(1:2)D	250	4.14	10.22
SCM75(1:2)E	248	4.72	10.85

Fibre-reinforced self-compacting mortars

Following the results of self-compatibility and compressive strength development, mix SCM75(1:1) and SCM(1:2) were considered to prepare the fibre-reinforced self-compacting mortars using the combination of basalt and polypropylene fibres according to the following nomenclature for SCM75 mixes.

- SCM75A(1:1), and SCM75A(1:2): 1.00 vol% polypropylene fibre and 0.00% basalt fibre
- fSCM75B(1:1), and SCM75B(1:2): 0.75 vol% polypropylene fibre and 0.25% basalt fibre
- SCM75C(1:1), and SCM75C(1:2): 0.50 vol% polypropylene fibre and 0.50% basalt fibre
- SCM75D(1:1), and SCM75D(1:2): 0.25 vol% polypropylene fibre and 0.75% basalt fibre
- SCM75E(1:1), and SCM75E(1:2): 0.00 vol% polypropylene fibre and 1.00% basalt fibre

Rheological properties of fibre-reinforced SCM75

The results of the mini-slump flow and mini-V, and V-funnel of fibre-reinforced SCM75(1:1) and SCM75(1:2) are reported in Tables 7 and 8. This mini-slump flow varies from 246 to 274 mm, which is consistent with the requirements of EFNARC guidelines and also with that reported in the literature [32]. From the experimental results, it can be concluded that the fresh properties of all SCM mixtures with the addition of polypropylene and basalt fibres meet the criteria of the EFNARC guidelines.

Compressive and flexural strength, DME of fibre-reinforced SCM(1:1) and (b) SCM(1:2)

The compressive strength of fibre-reinforced SCM(1:1) and SCM(1:2) is depicted in Fig. 11a, b. It can be observed that the fibres and combined fibres have a positive influence on the mechanical properties. The results show that using basalt/polypropylene fibres increases the compressive strength in both blends compared to samples without fibre. The fibre addition effect overcame the compressive strength from the second day. Some variations observed in the Figures could be attributed to measurement errors and can be expressed as standard deviations.

The variation of flexural strength at the same curing time cannot be linearly described as function of material composition (Fig.12a, b). The values are low and the effect of

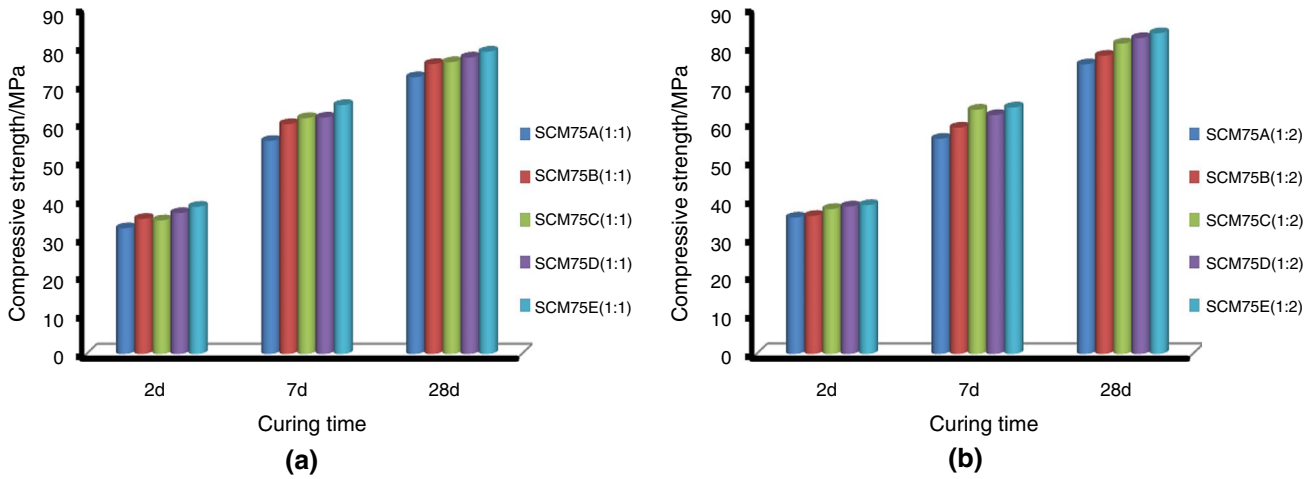

Figs.11 Compressive strength of **a** Fibre-reinforced SCM(1:1) and **b** SCM(1:2)

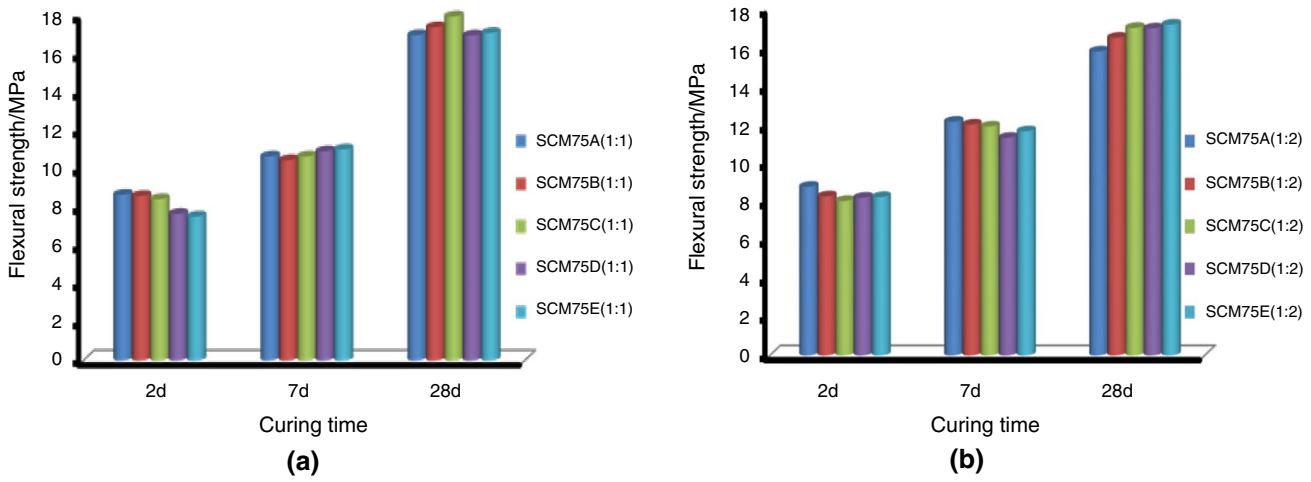

Fig.12 Flexural strength of **a** Fibre-reinforced SCM(1:1) and **b** SCM(1:2)

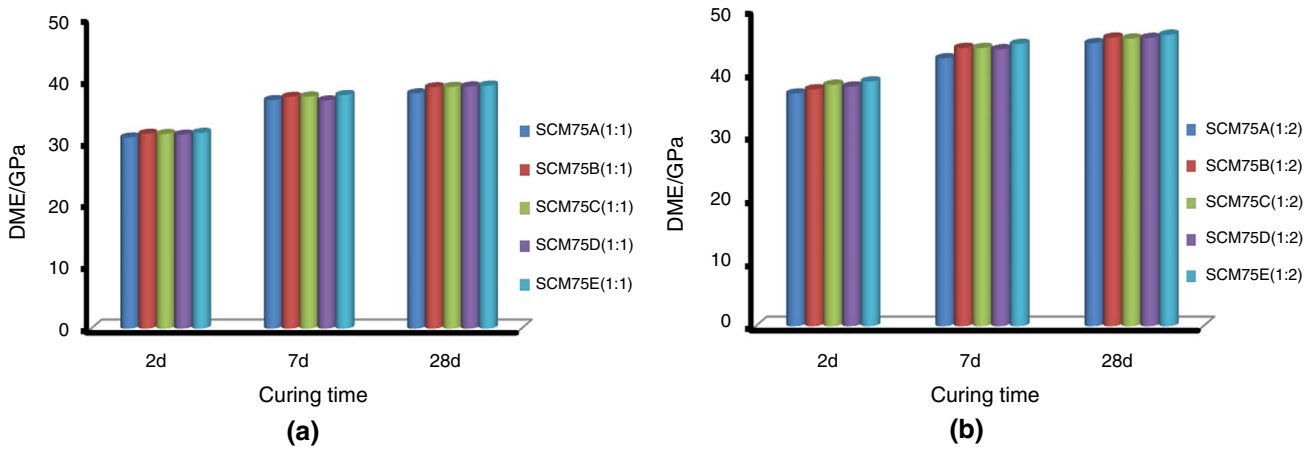

Fig.13 DME of **a** Fibre-reinforced SCM(1:1) and **b** Fibre-reinforced SCM(1:2)

standard deviation can explain these no uniform change. Nevertheless, the flexural strength increase with increasing curing time.

The DME of fibre-reinforced SCM(1:1) and SCM(1:2), calculated by measuring ultrasonic wave propagation velocity in the mortar, is depicted in Fig. 11a, b and varies from 30 to 50 GPa. The value increases with increasing curing time but slightly changes with the polypropylene/basalt fibre ratio. The DME of fibre-reinforced SCM is higher than that of the corresponding SCM75(1:1) and SCM75(1:2) without fibres. As concrete is a multiphase and heterogeneous material, the mechanical and physical properties, including the DME, depend on its material composition. Steel and fibre reinforcement is used to withstand the brittleness of concrete. Therefore, the presence of polypropylene and basalt fibres improves the elasticity properties of self-compacting mortars (Fig. 13)

Microstructure observations

Figure 14a–f depicts the micrographs of the selected self-compacting mortars. These are: control samples SCM100(1:1), SCM(1:2) with Portland cement; optimized material composition SCM75(1:1) and SCM75(1:2); fibre-reinforced SCM75A(1:1) and SCM75A(1:2) containing basalt fibre after 28-day curing. The visual observation clearly indicates that the microstructure changes with material compositions, filler content, and the presence of fibres. While using pure Portland cement leads to the formation of compact amorphous microstructure with needles resembling C–S–H, mortars of four-component binder present different microstructures showing the presence of large crystals covered by fine C–S–H or amorphous gel structure. The micrographs of SCM75a(1:1) and SCM75(1:2) are presented with a larger magnitude to observe the presence of fibres. The micrographs of

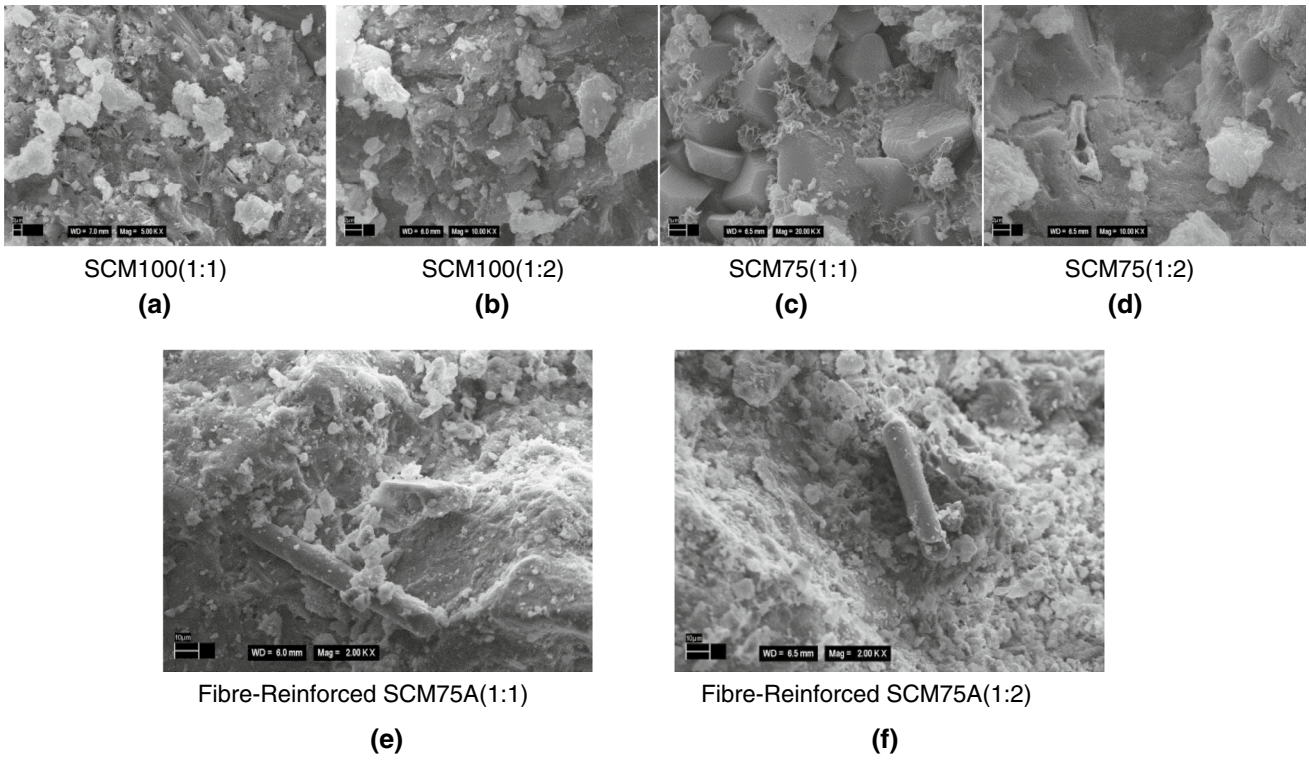

Figs. 14 Micrographs of selected self-compacting mortars (**a**, **b**, **c**, **d**) and fibre-reinforced self-compacting mortars (**e**, **f**)

SCM75a(1:1) and SCM75(1:2) are presented with a larger magnitude to observe the presence of fibres. With reduced amount of water and higher addition of superplasticizer, the microstructure of the fibre-reinforced self-compacting mortars seems to be denser than that of mortars without fibres. The microstructure images of the heterogeneous mortar system could be a matter of discussion as it is difficult to demonstrate the real representativeness of the entire system. However, this method is widely used by scientists to demonstrate the presence of crystalline hydrates, amorphous structures, and original non-hydrated phases. The method also makes it possible to focus on the interfacial transitional zone (ITZ) and other spaces to characterize the porous structure of mortars or concrete. When equipped with EDS, SEM allows elemental analysis of selected formations, which are often solid solutions.

Conclusions

Self-compacting mortars with two volumetric binder sand ratios of 1:1 and 1:2 (cement: sand) were developed based on the result of hydration heat, the material composition of the binder, and hybrid fibres. The composition of different mortars, including superplasticizer, was determined after several tests to meet the requirements of EFNARC for self-compacting mortars. Then, a combination of two fibres was used to prepare fibre-reinforced self-compacting mortars considering self-compacting mortars SCM75(1:1) and (SCM75(1:2) with the highest compressive. The hydration reaction in SCM mortars is influenced by the substitution levels of Portland cement by supplementary cementitious materials with the synergetic effect of pozzolanic activity leading to the enhancement of mortar performances (compressive and flexural strengths, dynamic modulus of elasticity) due to the formation of additional hydrated products. Up to 35% of substitution level, even SCM65(1:1) and SCM(1:2) have proved to have higher SAI than that required by the standard. Using hybrid fibres has also improved the mechanical properties of SCM. The microstructure has been found depending on material composition and the presence of fibres.

Acknowledgements This work was financially supported by the Slovak Research and Development Agency under the contracts APVV-19-0490, APVV-15-0631, as well as by Slovak Grant Agency VEGA under contracts 2/0080/24.

Author contributions SVR is a professor at National Institute of Technology, Department of Civil Engineering, Warangal, India. He has contributed by conception, leading the experimental works, analysing the data, and writing the manuscript. PM is senior researcher. He performed the experiments and analysed all data, and wrote the manuscript. RN is a senior research and has contributed by measuring

ad analysing the data obtained by calorimeter. JČ is a Ph.D. student and has contributed to the manuscript by establishing the grading curves, determining the mechanical and physical properties of concrete. ŽM is a young researcher at the Institute of Construction and Architecture from the Slovak Academy of Sciences. He contributed to the manuscript by measuring and analysing the data by Thermal Analysis Method. PC is a PhD student and has contributed by realizing the experimental works, analysing the data.

Funding Open access funding provided by The Ministry of Education, Science, Research and Sport of the Slovak Republic in cooperation with Centre for Scientific and Technical Information of the Slovak Republic. This work was supported by, Slovak Research and Development Agency APVV–15–0631, APVV-19-0490, and Slovak Grant Agency VEGA No. 2/0097/17,

Declarations

Conflict of interest The authors declare that they have no competing interests.

References

1. Dey S, Kumar VP, Goud KR, Basha SKJ. State of art review on self compacting concrete using mineral admixtures. J Build Pathol Rehabil. 2021;6(1):18. https://doi.org/10.1007/s41024-021-00110-9.
2. Felekoğlu B, Tosun K, Baradan B, Altun A, Uyulgan B. The effect of fly ash and limestone fillers on the viscosity and compressive strength of self-compacting repair mortars. Cem Concr Res. 2006;36:1719–26. https://doi.org/10.1016/j.cemconres.2006.04.002.
3. Türkel S, Altuntaş Y. The effect of limestone powder, fly ash and silica fume on the properties of self-compacting repair mortars. Sadhana. 2009;34:331–43. https://doi.org/10.1007/s12046-009-0011-3.
4. Mahdikhani M, Ramezanianpour AA. New methods development for evaluation rheological properties of self-consolidating mortars. Constr Build Mater. 2015;75:136–43. https://doi.org/10.1016/j.conbuildmat.2014.09.094.
5. Turk K. Viscosity and hardened properties of self-compacting mortars with binary and ternary cementitious blends of fly ash and silica fume. Constr Build Mater. 2012;37:326–34. https://doi.org/10.1016/j.conbuildmat.2012.07.081.
6. Benabed B, Kadri E, Azzouz L, Kenai S. Properties of self-compacting mortar made with various types of sand. Cem Concr Comp. 2012;34(10):1167–73. https://doi.org/10.1016/j.cemconcomp.2012.07.007.
7. Güneyisi E, Gesoğlu M. Properties of self-compacting mortars with binary and ternary cementitious blends of fly ash and metakaolin. Mater Struct. 2008;41:1519–31. https://doi.org/10.1617/s11527-007-9345-7.
8. Gesoğlu M, Güneyisi E, Özbay E. Properties of self-compacting concretes made with binary, ternary, and quaternary cementitious blends of fly ash, blast furnace slag, and silica fume. Constr Build Mater. 2009;23:1847–54. https://doi.org/10.1016/j.conbuildmat.2008.09.015.
9. Domone PL, Jin J. Properties of mortar for self-compacting concrete. In: Proceedings 1st international RILEM symposium on self-compacting concrete. Stockholm, Sweden; 1999. p. 109–20.
10. Kadhim AS, Atiyah AA, Salih SA. Properties of Self-compacting concrete containing nano cement kiln dust. Mater Today Proc. 2020;20(4):499–504. https://doi.org/10.1016/j.matpr.2019.09.177.
11. Santamaría A, González JJ, Losánez MM, Skaf M, Ortega-Lopéz V. The design of self-compacting structural mortar containing steelmaking slags as aggregate. Cem Concr Compos. 2020;111:103627–37. https://doi.org/10.1016/j.cemconcomp.2020.103627.
12. Abdolpour H, Niewiadomski P, Sadowski Ł, Kwiecień A. Engineering of ultra-high performance self-compacting mortar with recycled steel fibres extracted from waste tires. Arch Civ Mech Eng. 2022;22:175. https://doi.org/10.1007/s43452-022-00496-4.
13. Ramkumar KB, Kannan Rajkumar PR, Gunasekaran K. Performance of hybrid steel fiber-reinforced self-compacting concrete RC beam under flexure. Eng Sci Technol Int J. 2023;42:101432–45. https://doi.org/10.1016/j.jestch.2023.101432.
14. Li B, Chi Y, Xu L, Shi Y, Li Ch. Experimental investigation on the flexural behavior of steel-polypropylene hybrid fiber reinforced concrete. Constr Build Mater. 2018;191(10):80–94. https://doi.org/10.1016/j.conbuildmat.2018.09.202.
15. Koniki S, Prasad DR. Influence of hybrid fibres on strength and stress-strain behaviour of concrete under uni-axial stresses. Constr Build Mater. 2019;207:238–48. https://doi.org/10.1016/j.conbuildmat.2019.02.113.
16. Rios RT, Lolli F, Xie L, Xie Y, Kurtis KE. Screening candidate supplementary cementitious materials under standard and accelerated curing through time-series surface resistivity measurements and change-point detection. Cem Concr Res. 2021;148: 106538. https://doi.org/10.1016/j.cemconres.2021.106538.
17. Palou MT, Boháč M, Kuzielová E, Novotný R, Žemlička M, Dragomírová J. Use of calorimetry and thermal analysis to assess the heat of supplementary cementitious materials during the hydration of composite cementitious binders. J Therm Anal Calorim. 2020;142(1):97–117. https://doi.org/10.1007/s10973-020-09341-3.
18. Kuzielová E, Žemlička M, Novotný R, Palou MT. Simultaneous effect of silica fume, metakaolin and ground granulated blast-furnace slag on the hydration of multicomponent cementitious binders. J Therm Anal Calorim. 2019;136(4):1527–37. https://doi.org/10.1007/s10973-018-7813-7.
19. Rubinaite D, Dambrauskas T, Baltakys K, Siauciunas R. Investigation on the hydration and strength properties of belite cement mortar containing industrial waste. J Therm Anal Calorim. 2023;148:1481–90. https://doi.org/10.1007/s10973-022-11556-5.
20. Chaipanich A, Wianglor K, Piyaworapaiboon M, Sinthupinyo S. Thermogravimetric analysis and microstructure of alkali-activated metakaolin cement pastes. J Therm Anal Calorim. 2019;138:1965–70. https://doi.org/10.1007/s10973-019-08592-z.
21. Xu Z, Zhou Z, Du P, Cheng X. Effects of nano-limestone on hydration properties of tricalcium silicate. J Therm Anal Calorim. 2017;129:75–83. https://doi.org/10.1007/s10973-017-6123-9.
22. Wadsö L, Arndt M. An international round robin test on isothermal (conduction) calorimetry for measurement of three-day heat of hydration of cement. Cem Concr Res. 2016;79:316–22. https://doi.org/10.1016/j.cemconres.2015.10.004.

23. Luo X, Jiang X, Chen Q, Huang Z. An assessment method of hydration degree of rice husk ash blended cement considering temperature effect. Constr Build Mater. 2021;304: 124534. https://doi.org/10.1016/j.conbuildmat.2021.124534.
24. Dragomírová J, Palou MT, Kuzielová E, Žemlička M, Novotný R, Gméling K. Optimization of cementitious composite for heavyweight concrete preparation using conduction calorimetry. J Therm Anal Calorim. 2020;142(1):255–66. https://doi.org/10.1007/s10973-020-09530-0.
25. Talero R. Expansive synergic effect of ettringite from pozzolan (metakaolin) and from OPC, co-precipitating in a common plaster-bearing solution Part II: fundamentals, explanation and justification. Constr Build Mater. 2011;25(3):1139–58. https://doi.org/10.1016/j.conbuildmat.2010.09.006.
26. Homayoonmehr R, Ramezanianpour AA, Mirdarsoltany M. Influence of metakaolin on fresh properties, mechanical properties and corrosion resistance of concrete and its sustainability issues: a review. J Build Eng. 2021;44: 103011. https://doi.org/10.1016/j.jobe.2021.103011.
27. Nocuń-Wczelik W, Pacierpnik W, Kapeluszna E. Application of calorimetry and other thermal methods in the studies of granulated blast furnace slag from the old storage yards as supplementary cementitious material. J Therm Anal Calorim. 2022;147(15):8157–68. https://doi.org/10.1007/s10973-021-11161-y.
28. Kledyński Z, Machowska A, Pacewska B, Wilińska I. Investigation of hydration products of fly ash–slag pastes. J Therm Anal Calorim. 2017;130(1):351–63. https://doi.org/10.1007/s10973-017-6233-4.
29. Li C, Sun H, Li L. A review: The comparison between alkali-activated slag (Si+Ca) and metakaolin (Si+Al) cements. Cem Concr Res. 2010;40(9):1341–9. https://doi.org/10.1016/j.cemconres.2010.03.020.
30. The European guidelines for self-compacting concrete. Specification, production and use. The self-compacting concrete European project group (BIBM, CEMBUREAU, ERMCO, EFCA, EFNARC). 2005
31. Okamura H, Ozawa K. Mix design for self-compacting concrete. Concr Libr JSCE. 1995;25(6):107–20.
32. Nepomuceno M, Oliveira L. Parameters for self-compacting concrete mortar phase. ACI Mater J. 2008;253:323–40. https://doi.org/10.14359/20183.
33. Okamura H, Ouchi M. Self-compacting concrete. J Adv Concr Technol. 2003;1(1):5–15. https://doi.org/10.3151/jact.1.5.
34. Palou MT, Kuzielova E, Novotný R, Šoukal F, Žemlička M. Blended cements consisting of Portland cement–slag–silica fume–metakaolin system. J Therm Anal Calorim. 2016;125:1025–34. https://doi.org/10.1007/s10973-016-5399-5.
35. Záleská M, Pavlíková M, Pavlík Z, Jankovský O, Pokorný J, Tydlitát V, Svora P, Černý R. Physical and chemical characterization of technogenic pozzolans for the application in blended cements. Constr Build Mater. 2011;25(3):1139–58. https://doi.org/10.1016/j.conbuildmat.2017.11.021.